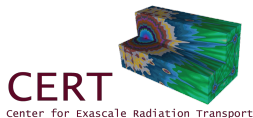


A High-Order Low-Order Algorithm with Exponentially-Convergent Monte Carlo for Thermal Radiative Transfer

Simon Bolding, Matt Cleveland, and Jim Morel

4 August 2016



We are interested in modeling thermal radiation transport in the high energy density physics regime

Modeling materials under extreme conditions

Temperatures $\mathcal{O}(10^6)$ K or more

Photon radiation transports through a material

Significant **energy** may be exchanged

We want to improve efficiency of Monte Carlo calculations

e.g., inertial confinement fusion, supernovae, et. al.

Our method has been applied to a simplified model:
the 1D frequency-integrated radiative transfer equations

Energy balance equations for radiation and material.

Radiation intensity $I(x, \mu, t)$, material temperature $T(x, t)$

$$\frac{1}{c} \frac{\partial I}{\partial t} + \mu \frac{\partial I}{\partial x} + \sigma_t I(x, \mu, t) = \frac{1}{4\pi} \sigma_a a c T^4,$$
$$C_v \frac{\partial T(x, t)}{\partial t} = \sigma_a \phi(x, t) - \sigma_a a c T^4$$

Equations are **nonlinear** and may be tightly coupled

Absorption opacity (σ_a) can be a strong function of T

Implicit Monte Carlo (IMC) is the standard Monte Carlo transport method for TRT problems

The system is *linearized* over a time step $t \in [t^n, t^{n+1}]$
Opacities are evaluated with $T(t^n)$

- ▶ Produces a linear transport equation
with effective emission and scattering terms
- ▶ MC particle histories are simulated
tallying radiation energy deposition
- ▶ Emission source is **not** fully time-implicit.
Uses MC integration over Δt for intensity

We developed a **high-order low-order (HOLo)** method that improves on several drawbacks of IMC

Standard IMC

Large **statistical noise** possible

Effective scattering can make MC very expensive

Linearization can cause **non-physical** results (maximum principle violations)

Reconstruction of linear emission shape limits artificial energy propagation

HOLo Method

ECMC is **very statistically efficient** for TRT problems

MC solution has **no scattering**

Fully **implicit** time-discretization and LO solution **resolves nonlinearities**

Linear-discontinuous FE for $T(x)$ preserving equilibrium diffusion limit

A HOLO Algorithm for Thermal Radiative Transfer



Overview of algorithm

Derivation of the LO equations

Exponentially Convergent MC High-Order Solver

Computational Results

Extensions and Ongoing Research

A HOLO Algorithm for Thermal Radiative Transfer



Overview of algorithm

Derivation of the LO equations

Exponentially Convergent MC High-Order Solver

Computational Results

Extensions and Ongoing Research

Basic idea is a nonlinear low-order system with high-order angular correction from Monte Carlo transport solves

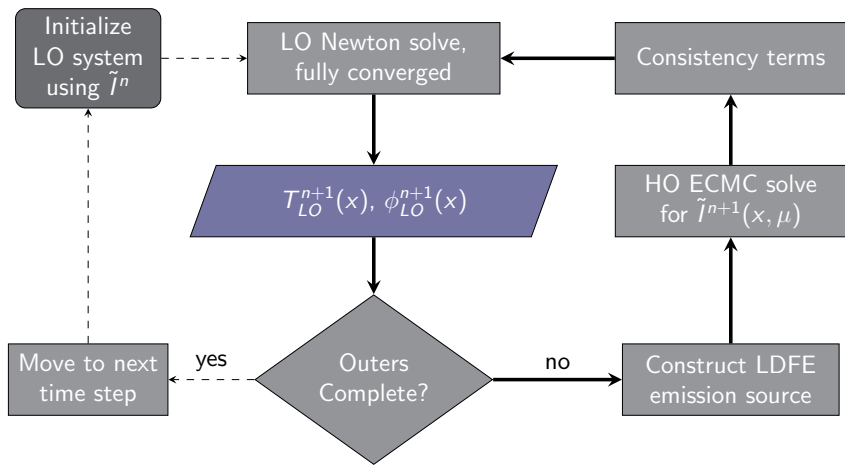
The **LO system** is space-angle moment equations, on a fixed finite-element (FE) spatial mesh

- ▶ Reduced dimensionality in angle
allows for solution with Newton's method
- ▶ **Output:** linear-discontinuous $\phi(x)$ and $T(x)$
Construct LDFE scattering and emission source

The **HO system** is a pure-absorber transport problem

- ▶ Solved with exponentially-convergent MC (ECMC)
for *efficient* reduction of statistical noise
- ▶ **Output:** consistency terms

Iterations between the HO and LO systems
can be performed each time step



A HOLO Algorithm for Thermal Radiative Transfer



Overview of algorithm

Derivation of the LO equations

Exponentially Convergent MC High-Order Solver

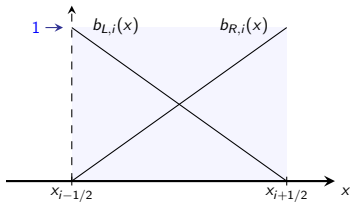
Computational Results

Extensions and Ongoing Research

The LO equations are formed as *consistently* as possible with spatial and angular moments of TRT equations

The time discretization is backward Euler
for both the HO and LO equations

Spatial moments are weighted with FE basis functions:



$$\langle \cdot \rangle_{L,i} = \frac{2}{h_i} \int_{x_{i-1/2}}^{x_{i+1/2}} b_{L,i}(x)(\cdot) dx$$

Half-range integrals reduce angular dimensionality

$$I^+(x) = 2\pi \int_0^1 I(x, \mu) d\mu$$

Apply moments to the TRT equations
and manipulate to form **angular consistency terms**

For example, apply $\langle \cdot \rangle_{L,i}^+$ to a streaming term:

$$\begin{aligned} \left\langle \mu \frac{\partial I}{\partial x} \right\rangle_L^+ &= -\frac{2}{h_i} \{\mu I\}_{i-1/2}^+ + \frac{1}{h_i} [\langle \mu I \rangle_{L,i}^+ + \langle \mu I \rangle_{R,i}^+] \\ &= -\frac{2}{h_i} \frac{\{\mu I\}_{i-1/2}^+}{I_{i-1/2}^+} I_{i-1/2}^+ + \frac{1}{h_i} \frac{\langle \mu I \rangle_{L,i}^+}{\langle I \rangle_{L,i}^+} \langle I \rangle_{L,i}^+ + \frac{1}{h_i} \frac{\langle \mu I \rangle_{R,i}^+}{\langle I \rangle_{R,i}^+} \langle I \rangle_{R,i}^+ \end{aligned}$$

Apply moments to the TRT equations
and manipulate to form **angular consistency terms**

For example, apply $\langle \cdot \rangle_{L,i}^+$ to a streaming term:

$$\begin{aligned} \left\langle \mu \frac{\partial I}{\partial x} \right\rangle_L^+ &= -\frac{2}{h_i} \{\mu I\}_{i-1/2}^+ + \frac{1}{h_i} [\langle \mu I \rangle_{L,i}^+ + \langle \mu I \rangle_{R,i}^+] \\ &= -\frac{2}{h_i} \frac{\{\mu I\}_{i-1/2}^+}{I_{i-1/2}^+} I_{i-1/2}^+ + \frac{1}{h_i} \frac{\langle \mu I \rangle_{L,i}^+}{\langle I \rangle_{L,i}^+} \langle I \rangle_{L,i}^+ + \frac{1}{h_i} \frac{\langle \mu I \rangle_{R,i}^+}{\langle I \rangle_{R,i}^+} \langle I \rangle_{R,i}^+ \end{aligned}$$

Now, close the final moment equations:

- Approximate consistency terms with \tilde{I}_{HO}^{n+1}
from previous HO solve
- Eliminate remaining face unknowns with LD spatial closure
 $T^4(x)$ and $T(x)$ also assumed LD

A HOLO Algorithm for Thermal Radiative Transfer



Overview of algorithm

Derivation of the LO equations

Exponentially Convergent MC High-Order Solver

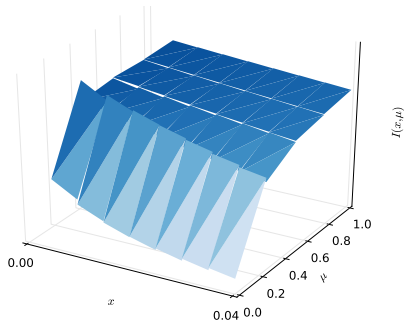
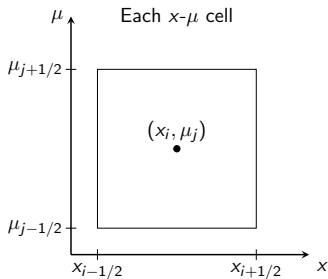
Computational Results

Extensions and Ongoing Research

We use a **projection** $\tilde{I}(x, \mu)$ onto a space-angle LDFF mesh to represent the solution

local volumetric tallies

$$\tilde{I}_{ij}(x, \mu) = I_a + \frac{2}{h_x} I_x (x - x_i) + \frac{2}{h_\mu} I_\mu (\mu - \mu_i)$$



We apply the ECMC algorithm to the **pure-absorber** HO transport equation

$$\left[\mu \frac{\partial}{\partial x} + \left(\sigma_t + \frac{1}{c \Delta t} \right) \right] I^{n+1} = \frac{1}{4\pi} \left[\sigma_a a c (T_{LO}^{n+1})^4 + \sigma_s \phi_{LO}^{n+1} \right] + \frac{\tilde{I}^n}{c \Delta t}$$
$$\mathbf{L} I^{n+1} = q$$

For each batch m :

- ▶ Evaluate residual source: $r^{(m)} = q - \mathbf{L} \tilde{I}^{n+1,(m)}$
- ▶ Estimate $\epsilon^{(m)} = \mathbf{L}^{-1} r^{(m)}$ via **MC simulation**
- ▶ Update solution: $\tilde{I}^{n+1,(m+1)} = \tilde{I}^{n+1,(m)} + \tilde{\epsilon}^{(m)}$

Our HO system allows for straight-forward variance reduction and source biasing

$I^n(x, \mu)$ is often an **excellent** estimate of $I^{n+1}(x, \mu)$
No MC sampling from thermal equilibrium regions

Histories stream without collision
along path s , weight reduces as $w(s) = w_0 e^{-\sigma_t s}$

Use cell-wise systematic sampling for $|r^{(m)}|$ source
Particularly effective in thick cells

- ▶ Particles in each x - μ cell $\propto |r^{(m)}|$ in cell
- ▶ Set minimum n for cells
except for cells in thermal equilibrium

A HOLO Algorithm for Thermal Radiative Transfer



Overview of algorithm

Derivation of the LO equations

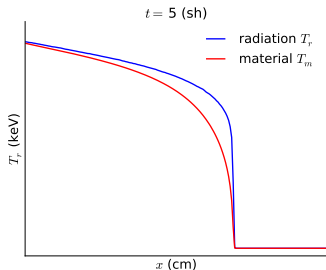
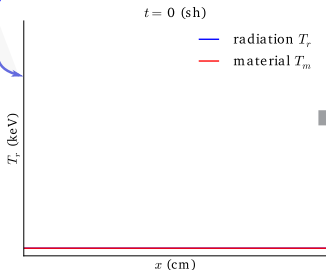
Exponentially Convergent MC High-Order Solver

Computational Results

Extensions and Ongoing Research

We will test our method with several standard **Marshak Wave** problems

constant radiation
boundary source



Figures depict radiation temperature $T_r = \sqrt[4]{\phi/ac}$

Implementation specifics for results are given below:

- ▶ HOLO method implemented as stand-alone C++ code
IMC results from Jayenne (LANL code)
- ▶ Δt increases from 0.01 ns to 0.1 ns
- ▶ One HO solve per time step, with two LO solves
 - ▶ *each HO solve* has 3 ECMC batches
no adaptive mesh refinement

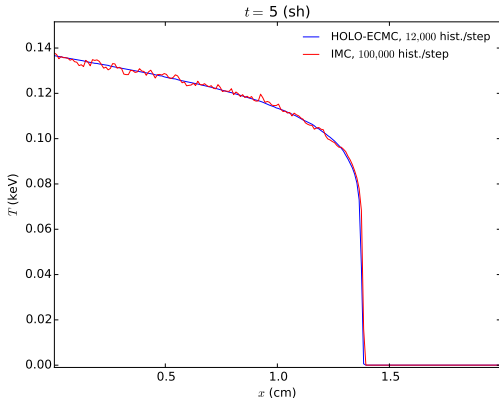
▶ Figure of Merit:
$$\text{FOM} = \frac{1}{\|\sigma_{\text{rel}}\|^2 N_{\text{total}}}$$

are normalized to IMC results

The HOLO method produces significantly less noise than IMC for a typical Marshak Wave: **FOM=145**

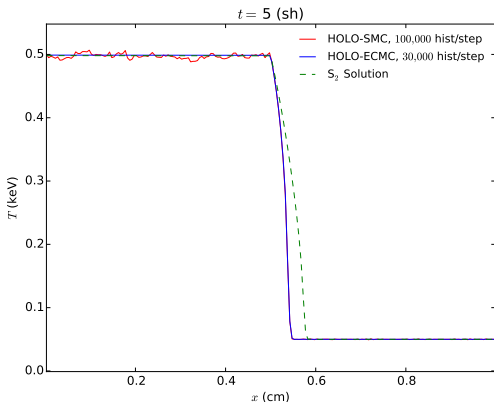
► $\sigma_a \propto T^{-3}$

- Transient solution after 5 shakes (~ 520 steps)
200 x cells (and 4 μ cells for ECMC)



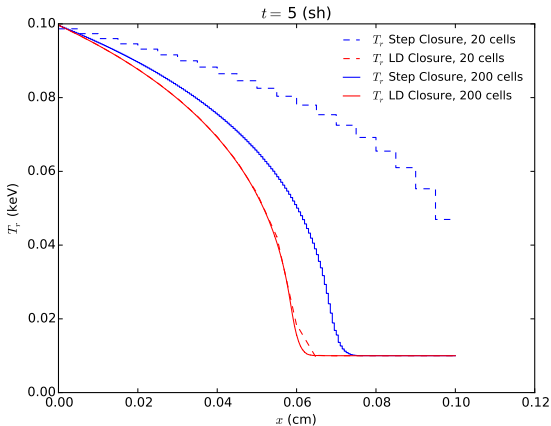
ECMC is more efficient than standard MC as a HO solver

- ▶ Left half is optically thin ($\sigma=0.2 \text{ cm}^{-1}$), right half is thick ($\sigma_a=2000 \text{ cm}^{-1}$). 8μ cells
- ▶ Results for HOLO with different HO solvers:
ECMC (FOM=10,000), standard MC (FOM=0.46), and an S_2 solution



The LDFE discretization for the LO equations preserves the equilibrium diffusion limit

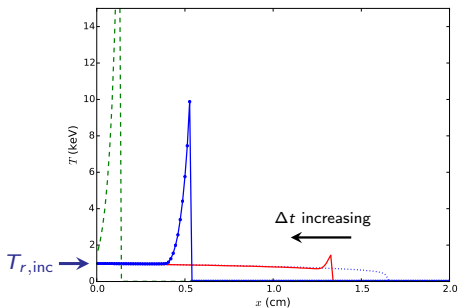
- Large, constant σ_a and small c_v



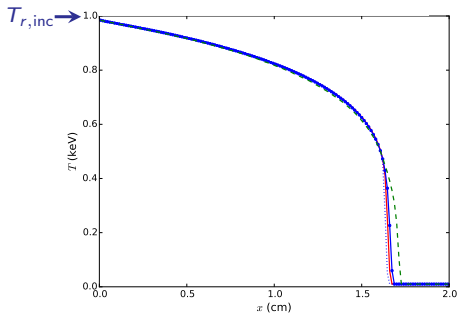
Our HOLO method preserves the maximum principle with sufficient nonlinear convergence

- ▶ **Material temperatures** plotted; all simulations end at $t = 0.1$ sh
 $\sigma_a \propto T^{-3}$, c_v small, $\Delta t \in [10^{-4}, 10^{-2}]$ sh
- ▶ LO Newton iterations required damping

IMC T_m



HOLO T_m



A HOLO Algorithm for Thermal Radiative Transfer



Overview of algorithm

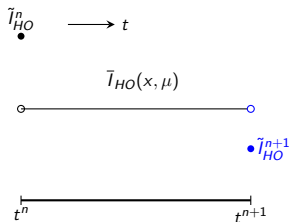
Derivation of the LO equations

Exponentially Convergent MC High-Order Solver

Computational Results

Extensions and Ongoing Research

The time variable can be included in the ECMC trial space with a consistent LO time closure



Include continuous $\frac{1}{c} \frac{\partial}{\partial t} (\cdot)$ in \mathbf{L} for residual source leaving $T(x)$ still implicit

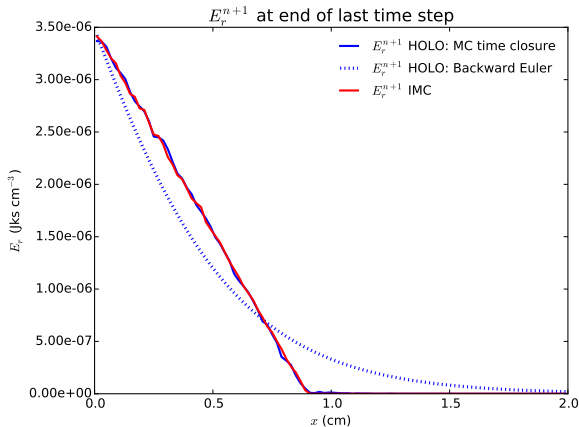
Sample and track particle histories in time.
Tally the time-averaged and t^{n+1} error

In **LO equations**, parameterize ϕ_{LO}^{n+1} in terms of **time-averaged** unknowns, e.g.,

$$\langle \phi \rangle_{L,i}^{n+1} = 2 \gamma_{L,i}^{HO} \overline{\langle \phi \rangle}_{L,i} - \langle \phi \rangle_{L,i}^n$$

The time-closure parameters preserve accuracy of MC time integration in the LO solution

- ▶ Material has $\sigma_a = 10^{-6} \text{ cm}^{-1}$, so temperature uncouples
take 3 large time steps and compare $E_R^{n+1} = \phi^{n+1}/c$
- ▶ 300,000 histories/step, 100 spatial cells, **FOM=0.53**

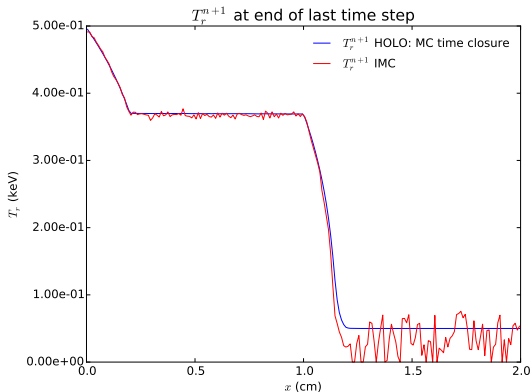


With sufficient histories in a mix of optical thicknesses HOLON is more efficient than IMC

- ▶ 3 Material regions: $\sigma_a = 100 \text{ cm}^{-1}$, $\sigma_a = 0.01 \text{ cm}^{-1}$, $\sigma_a = 100 \text{ cm}^{-1}$.
- ▶ 10^6 histories per time step, 200 cells, $t = 2 \text{ sh}$

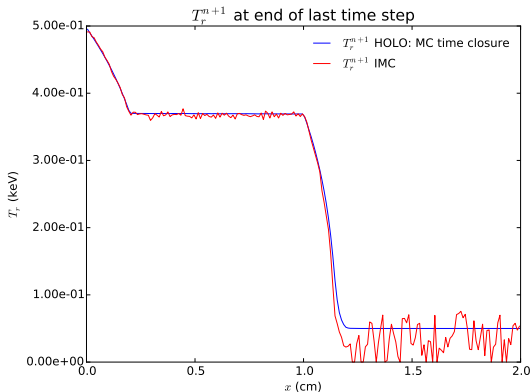
With sufficient histories in a mix of optical thicknesses HOLO is more efficient than IMC

- ▶ 3 Material regions: $\sigma_a = 100 \text{ cm}^{-1}$, $\sigma_a = 0.01 \text{ cm}^{-1}$, $\sigma_a = 100 \text{ cm}^{-1}$.
- ▶ 10^6 histories per time step, 200 cells, $t = 2 \text{ sh}$



With sufficient histories in a mix of optical thicknesses HOLO is more efficient than IMC

- ▶ 3 Material regions: $\sigma_a = 100 \text{ cm}^{-1}$, $\sigma_a = 0.01 \text{ cm}^{-1}$, $\sigma_a = 100 \text{ cm}^{-1}$.
- ▶ 10^6 histories per time step, 200 cells, $t = 2 \text{ sh}$



- ▶ HOLO with Backward Euler has same temporal accuracy, but better statistics for this problem

A few other potential improvements were investigated:

Resolving negative intensities in optically thick cells
using an artificial source and alternate trial space

Using HO solution to estimate spatial closure
by including face tallies in ECMC

Source iteration with diffusion synthetic acceleration
to iteratively solve the LO equations

A HOLO Algorithm for Thermal Radiative Transfer

ECMC is very efficient for TRT simulations
and fits well in global HOLO method

The LO system can resolve nonlinearities
with bounded angular consistency terms

Next step is to extend to higher dimensions
main hurdle to overcome is infrastructure

A HOLO Algorithm for Thermal Radiative Transfer

ECMC is very efficient for TRT simulations
and fits well in global HOLO method

The LO system can resolve nonlinearities
with bounded angular consistency terms

Next step is to extend to higher dimensions
main hurdle to overcome is infrastructure

More details in: S.R. Bolding, M. Cleveland, and J.E. Morel. A HOLO Algorithm with ECMC for Radiative Transfer. NS&E: M&C 2015 Special Issue, 2016. Accepted.

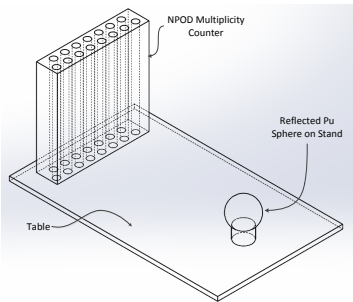
Simulations of Neutron Multiplicity Experiments with Perturbations to Nuclear Data

Simon Bolding and C.J. Solomon

4 August 2016



Multiplicity experiments were performed for validating subcritical simulations



*Not to scale

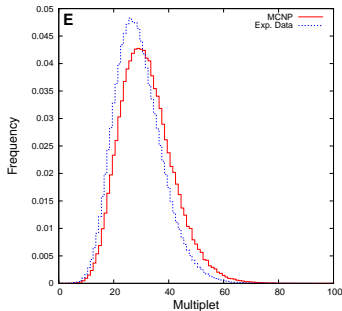
Experimental Parameters

- ▶ 94% ^{239}Pu sphere
- ▶ 5 reflector configurations
None to 3.0 cm HDPE shells

Experiments repeated w/ ^{252}Cf

C.J. Solomon modeled experiments with modified MCNP5

MCNP5 simulated multiplicity distributions showed discrepancy with experiments for Pu, but not for ^{252}Cf



Pu with 3.0-cm HDPE reflector

Previous work by Mattingly [2010]

- Caused by ^{239}Pu nuclear data
- Decreased energy-integrated $\bar{\nu}$,
 $\bar{\nu}$: mean # of neutrons/fission

ENDF-VII raised $\bar{\nu}$ for ^{239}Pu
to match k_{eff} benchmarks

- $\bar{\nu}$ is $\sim 2\sigma$ above measured data
for $E < 1.5$ MeV

Can we reduce discrepancy in multiplicity distributions without significantly altering k_{eff} ?

Perform energy-dependent perturbations of $\bar{\nu}(E)$ in ^{239}Pu
Random samples drawn from ENDF-VII.1 covariance data

Compare experimental and simulated multiplicity dist.
and a k_{eff} benchmark (Jezebel)

Compare $\bar{\nu}(E)$ results to uniform shifts of microscopic cross sections

LANL Python nuclear data library was modified to generate energy-dependent $\bar{\nu}$ samples

1. Generate a correlated sample of $\bar{\nu}(E)$
 - ▶ Assumed multivariate Gaussian
with group-averaged covariances
2. Modify continuous $\bar{\nu}(E)$ data in **ACE** file
3. Perform all MCNP simulations
with modified ACE data

A cost function provides a measure of inaccuracy for each data realization

Reduced χ^2 values for the 5 multiplicity experiments and criticality benchmark

$$\chi_{\text{red,mult},m}^2 = \frac{1}{N_{\text{bins}} - 1} \sum_{i=1}^{N_{\text{bins}}} \frac{(P_i^{\text{exp}} - P_i^{\text{mcnp}})^2}{\sigma^2(P_i^{\text{exp}}) + \sigma^2(P_i^{\text{mcnp}})}$$

Equally weight χ^2 values in a **cost** function
A lower score indicates higher accuracy

$$\text{Cost} = \sum_{m=1}^5 \chi_{\text{red,mult},m}^2 + \chi_{\text{red},k_{\text{eff}}}^2$$

Multiplicity and k_{eff} simulations were performed for 500 unique realizations of $\bar{\nu}$ data

Trial	Cost	$\chi^2_{k_{\text{eff}}}$
$\bar{\nu}$ -1.14%	164.24	33.66
303	197.07	4.18
55	267.9	0.01
Original	426.86	0.27

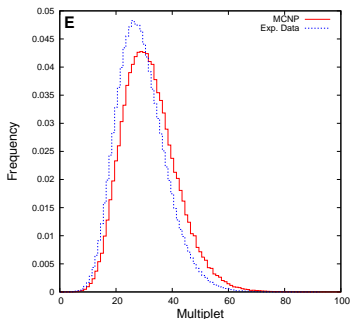
MCNP criticality test suite performed for best data which includes 39 criticality benchmarks w/ ^{239}Pu :

Trial	<i>RMSD</i>
$\bar{\nu}$ -1.14%	1.23%
303	0.51%
Original	0.49%

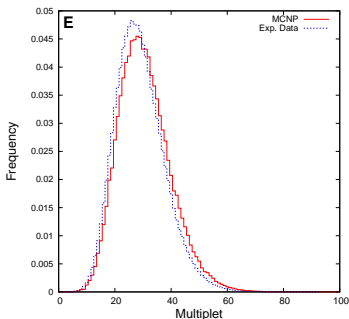
Energy-dependent $\bar{\nu}$ perturbations improved all 5 multiplicity distributions

- Plots for best data realization and 3.0 cm HDPE case

Original $\bar{\nu}$ Data



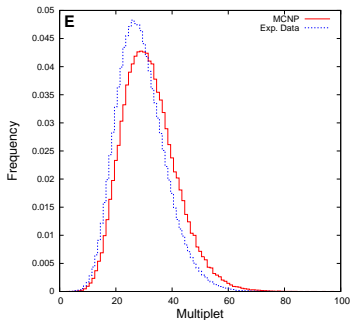
Trial 303: Lowest Cost



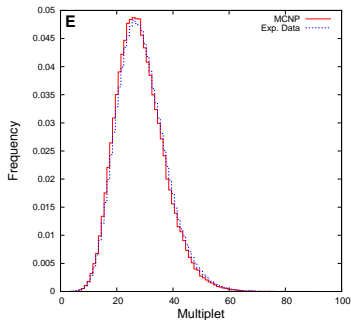
- Best data set reduced **bias** in 1st and 2nd moments, averaged over all 5 simulations, by \sim **35%**

Adjusting the fission cross section **uniformly**
showed good correction to multiplicity simulations

Original σ_f Data



σ_f decreased 1.5%



- High accuracy for all simulations: $\sum_{i=1}^5 \chi_{red,mult,m}^2 = 14.6$
- k_{eff} is **not** preserved: $\chi_{k_{eff}}^2 = 22.6$

Simulations of Multiplicity Experiments with Nuclear Data Perturbations

Energy-dependent $\bar{\nu}$ perturbations reduced inaccuracies
in multiplicity while preserving k_{eff}

- ▶ Majority of cross-correlation terms $\mathcal{O}(10^{-4})$ or less
- ▶ σ_f may need more investigation
not sensitive to capture cross section

Subcritical simulations should be considered
in validation of nuclear data

Next step is to extend methodology
for evaluating nuclear data

More details for nuclear data uncertainty work in

S.R. Bolding and C.J. Solomon. Simulations of Multiplicity Distributions with Perturbations to Nuclear Data. Proceedings, ANS Winter Meeting, 2013.

A radiation-hydrodynamics project I did not discuss today was recently submitted to JCP:

S.R. Bolding, J. Hansel, R.B. Lowrie, J.D. Edwards, and J.E. Morel. Second-Order Discretization in Space and Time for Radiation-Hydrodynamics. Journal of Computational Physics, 2016. *Submitted*.

Simulations of Neutron Multiplicity Experiments with Nuclear Data Perturbations

S.R. Bolding¹, C.J. Solomon²

¹ *Texas A&M University, College station, TX*

² *Los Alamos National Laboratory, Los Alamos, NM*

4 August 2016



Backup Slides

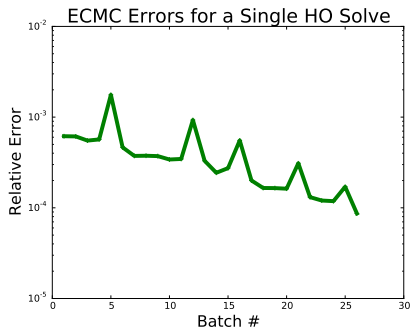
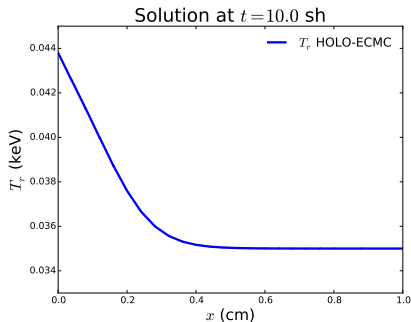
S.R. Bolding¹, C.J. Solomon²

¹ *Texas A&M University, College station, TX*

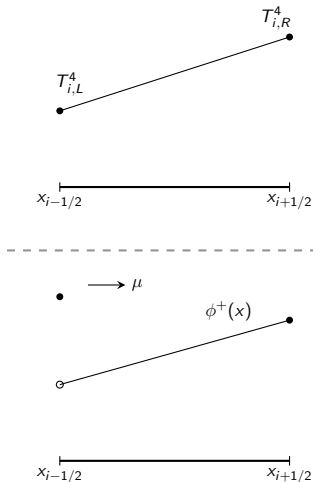
² *Los Alamos National Laboratory, Los Alamos, NM*



Exponential convergence can be maintained if the LDFFE mesh resolves the solution reasonably



We can close equations with HO angular information and a linear-discontinuous (LD) spatial discretization



1. Assume $T(x)$ and $T^4(x)$ are LD

2. A lagged $\tilde{I}_{\text{HO}}^{n+1}$ is used to evaluate consistency terms

3. Eliminate $\phi_{i+1/2}^\pm$ with LD closure preserving equi. diff. limit

$$\phi_{i+1/2}^+ = 2\langle\phi\rangle_{R,i}^+ - \langle\phi\rangle_{L,i}^+$$

4. Global system solved with Newton's method and lagged **implicit opacities**
Energy is always conserved

We need a way to resolve issues when the LDFF representation of the intensity is negative

Negative intensities can occur in optically thick cells
Mesh refinement is of minimal use

$\tilde{I}_{HO}(x, \mu)$ must be positive for consistency terms
to produce a physical, stable LO solution

Independent fix up for LO solution

E.g., lumping or preserving balance with floored $\phi(x)$

Can add source δ to produce a positive projection \tilde{l}_{pos} such that \tilde{l}_{pos} satisfies the latest residual equation

Produce \tilde{l}_{pos} by scaling $x - \mu$ moments equally,
to estimate source for the next iteration

$$\begin{array}{lcl} \mathbf{L}\tilde{l}^{(m)} = q - r^{(m)} & \longrightarrow & \delta^{(m+1)} = \mathbf{L} \left(\tilde{l}^{(m)} - \tilde{l}_{pos}^{(m)} \right) \\ \mathbf{L}\tilde{l}_{pos}^{(m)} = q - r^{(m)} + \delta^{(m+1)} & & q \rightarrow q + \delta^{(m+1)} \end{array}$$

We can delay error stagnation

Investigating alternative positive projection of l

Solving LO System with Newton's Method

- Linearization:

$$\underline{B}(T^{n+1}) = \underline{B}(T^*) + (T^{n+1} - T^*) \left. \frac{\partial \underline{B}}{\partial t} \right|_{t^*}$$

- Modified system

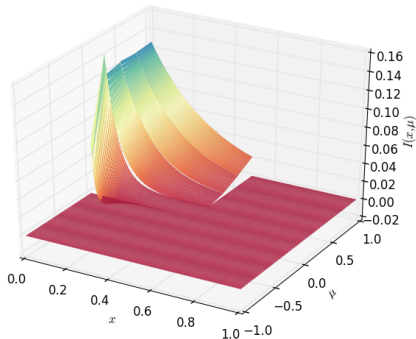
$$[\mathbf{D}(\mu^\pm) - \sigma_a^*(1 - f^*)] \underline{\Phi}^{n+1} = f^* \underline{B}(T^*) + \frac{\underline{\Phi}^n}{c\Delta t}$$

$$\hat{\mathbf{D}} \underline{\Phi}^{n+1} = \underline{Q}$$

$$f = \left(1 + \sigma_a^* c \Delta t \frac{4aT^{*3}}{\rho c_v} \right)^{-1} \quad T_i^* = \frac{T_{L,i}^* + T_{R,i}^*}{2}$$

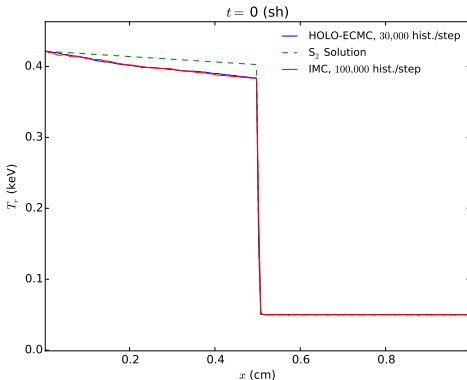
- Equation for T^{n+1} based on linearization that is conservative
- Converge T^{n+1} and $\langle \phi \rangle$ with Newton Iterations

The angular flux for the two material problem is difficult to resolve near $\mu = 0$



Two Material Problem, comparison in optically thin region

- Plot of radiation temperature after 10 time steps



Backup slide with timing results

Forming the LO System

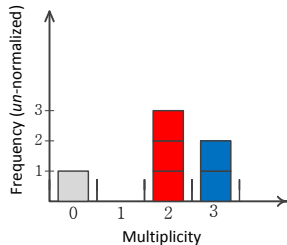
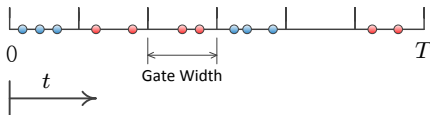
- Taking moments of TE yields 4 equations, per cell i , e.g.

$$\begin{aligned} & -2\mu_{i-1/2}^{n+1,+} \phi_{i-1/2}^{n+1,+} + \{\mu\}_{L,i}^{n+1,+} \langle \phi \rangle_{L,i}^{n+1,+} + \{\mu\}_{R,i}^{n+1,+} \langle \phi \rangle_{R,i}^{n+1,+} + \\ & \left(\sigma_t^{n+1} + \frac{1}{c\Delta t} \right) h_i \langle \phi \rangle_{L,i}^{n+1,+} - \frac{\sigma_s h_i}{2} \left(\langle \phi \rangle_{L,i}^{n+1,+} + \langle \phi \rangle_{L,i}^{n+1,-} \right) \\ & = \frac{h_i}{2} \langle \sigma_a^{n+1} a c T^{n+1,4} \rangle_{L,i} + \frac{h_i}{c\Delta t} \langle \phi \rangle_{L,i}^{n,+}, \quad (1) \end{aligned}$$

- Cell unknowns: $\langle \phi \rangle_{L,i}^+$, $\langle \phi \rangle_{R,i}^+$, $\langle \phi \rangle_{L,i}^-$, $\langle \phi \rangle_{R,i}^-$, T_L , T_R
- Need angular consistency terms and spatial closure (LD)

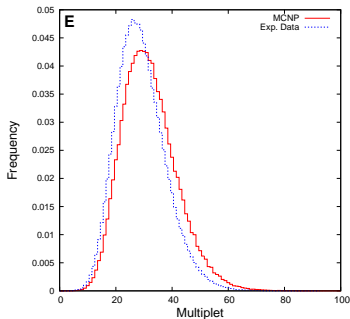
Neutron multiplicity distributions provide passive multiplication information about a fissionable system

○ = Detected Neutron

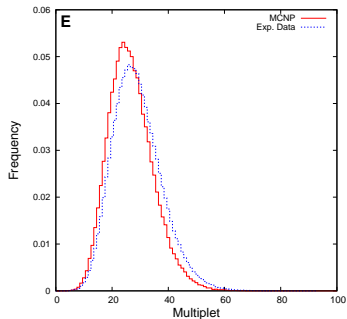


Energy-Integrated $\bar{\nu}$ Shift – 3.0 cm HDPE reflector

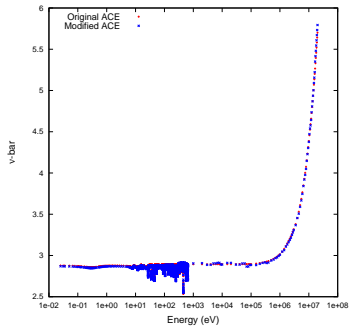
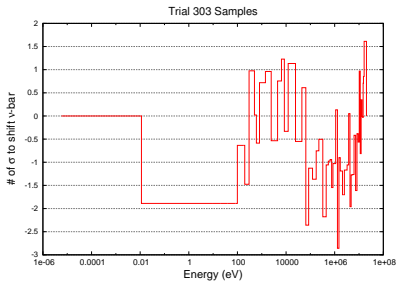
Original $\bar{\nu}$ Data



-1.14% $\bar{\nu}$ Data



The best $\bar{\nu}$ data (trial 303)



Fractional shifts to cross sections were made for comparison

Adjusted cross section uniformly at all energies
compensated with σ_{tot} or σ_{el}

Increasing capture cross section was not effective
relative to variance in data

Scaling fission cross section 1.5% ($< 1\sigma$)
improved multiplicity distributions

- ▶ Adjust elastic scattering (σ_{el}) to compensate change in σ_f , for $E > 1$ keV
- ▶ Better improvement than *uniform* scaling of $\bar{\nu}$